EMITTANCE AND MOMENTUM DIAGNOSTICS FOR BEAMS WITH LARGE MOMENTUM SPREAD

M. Olvegård* and V. Ziemann, Uppsala University, Sweden

Abstract

Commonly used beam diagnostic methods, such as spectrometry or emittance measurements through quadrupole scans, are based on the assumption that the beam momentum spread is very small. This assumption is sometimes not fulfilled, which leads to a systematic misinterpretation of the measurement. We have studied this effect and present algorithms that consider the full momentum distribution and offer correct ways of analyzing the profile measurements.

INTRODUCTION

In modern particle accelerators, like the Compact Linear Collider, CLIC [1], or plasma wakefield accelerators [2], the beam can have a significant momentum spread on the order of tens of percent. Conventional diagnostic methods, on the other hand, often assume a beam with no or very small momentum spread [3], which may lead to a systematic misinterpretation of the measurements. For example, emittance measurements based on quadrupole scan or multiple screen measurements, and momentum profile measurements through spectrometry, rely on determining the beam size, while the evolution of the beam envelope depends on the beam momentum distribution. We have studied the systematic errors that arise and developed novel algorithms to correctly analyze these measurements for arbitrary momentum distributions. As an application we consider the CLIC drive beam decelerator, where extraction of up to 90% of the kinetic energy leads to a very large momentum spread. We study a measurement of the time-resolved momentum distribution, based on sweeping the beam in a circular pattern to determine the momentum distribution and recording the beam size on a screen using optical transition radiation. We present the algorithm to extract the time-resolved momentum distribution, together with simulation results to prove its applicability.

SPECTROMETRY

Consider the spectrometer line depicted in Fig. 1. An incoming particle with momentum deviation $\delta = \Delta p/p_0$, where the index 0 refers to an on-momentum particle, is deflected an angle $\varphi(\delta)$ by a dipole magnet and detected on a screen or a similar profile monitor at the distance L from the center of the magnet. In the plane of deflection the particle coordinate on the screen is given by

$$X = L\varphi(\delta) = \frac{L\varphi_0}{1+\delta}\,. \tag{1}$$

* maja.olvegard@physics.uu.se

The incoming momentum distribution $\psi(\delta)$ is obtained by measuring the spatial distribution $\Psi(X)$ on a screen or similar profile monitor in the spectrometer and then translating back to momentum through Eq. (1). If the momentum spread is small, i.e. if $\delta << 1$, then the linear approximation $X = L\varphi_0/(1+\delta) \approx L\varphi_0(1-\delta)$ can be applied and the dispersion function $D = L\varphi_0$ can be used for the transformation between momentum distribution and spatial distribution. Here, we look at cases where δ is not small, which means that the full nonlinear relation in Eq. (1) must be used.

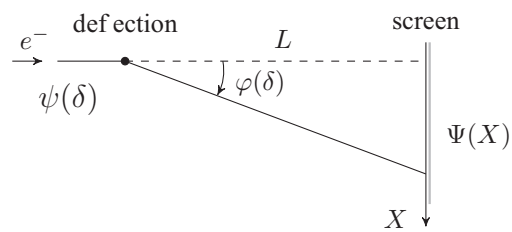

Figure 1: Schematic of a spectrometer line and associated variables.

Now we consider an arbitrary beam momentum distribution $\psi(\delta)$ and calculate the corresponding spatial distribution on the spectrometer screen. The particle density at a given position X is obtained by summing over all momenta, weighted by the momentum distribution, and make use of the relation in Eq. (1). We obtain

$$\begin{aligned}\Psi(X) &= \int \psi(\delta)\delta_D\left(X - \frac{L\varphi_0}{1+\delta}\right)d\delta \\ &= \frac{L\varphi_0}{X^2}\Psi\left(\frac{L\varphi_0 - X}{X}\right)\end{aligned} \tag{2}$$

where δ_D denotes the Dirac delta function. The factor $L\varphi_0/X^2$ appears in the change of coordinate in the integration. At the singularity $X \to 0$, which is equivalent to infinite momentum, the particle density is enhanced. An example is shown in Fig. 2 where three Gaussian momentum distributions

$$\psi(\delta) = \frac{1}{\sqrt{2\pi}\Delta}\exp\left(-\frac{\delta^2}{2\Delta^2}\right) \tag{3}$$

with rms width $\Delta = 0.05,\ 0.10,\ 0.15$ have been translated into spatial distributions in a spectrometer with $L\varphi_0 = 0.3\,\mathrm{m}$. As the momentum spread grows the Gaussian gets deformed. If the linear approximation is used for extracting the momentum distribution the profile is misinterpreted towards a higher average momentum and a smaller momentum spread. For more details, see Ref. [4].

ISBN 978-3-95450-127-4

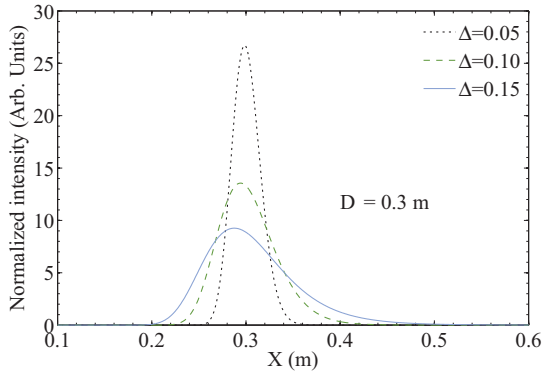

Figure 2: Important to note here is that if the screen distribution is converted to momentum distribution using the linear approximation the result will be higher average momentum and a smaller spread than what is true.

However, if the momentum spread is known to be large we can correctly extract momentum information from the spatial profile $\Psi(X)$ through the inverse procedure

$$\psi(\delta) = \int \Psi(X)\delta_D\left(\delta - \frac{L\varphi_0 - X}{X}\right)d\delta = \frac{L\varphi_0}{(1+\delta)^2}\psi\left(\frac{L\varphi_0}{1+\delta}\right). \quad (4)$$

Note that this is an analytical derivation of a non-perturbative method to analyze spectrometer measurements which is valid for arbitrary momentum distributions. Now that we have shown how to correctly measure the momentum distribution through spectrometry we will go into how the large momentum spread affects other beam diagnostic methods.

EMITTANCE MEASUREMENTS

We consider a measurement of the beam Twiss parameters through a quadrupole scan measurement. In a quadrupole scan the transverse beam size is measured during the systematic shift of the strength of an upstream located quadrupole magnet. If R is the transfer matrix of the beam line from the quadrupole to the beam size measurement the beam size Σ can be expressed as

$$\Sigma^2 = R_{11}^2\sigma_{11} + 2R_{11}R_{12}\sigma_{12} + R_{12}^2\sigma_{22} \quad (5)$$

where σ_{ij} are the incoming beam parameters that are to be determined. The transfer matrix elements R_{ij} depend on the focusing strength k of the quadrupole magnet, and with several measurements, for different values of k, a system of equations linear in σ_{ij} is built up. We determine the incoming parameters by solving this system of equations and calculate the Twiss parameters through

$$\varepsilon^2 = \sigma_{11}\sigma_{22} - \sigma_{12}^2, \quad \beta = \frac{\sigma_{11}}{\varepsilon}, \quad \alpha = -\frac{\sigma_{12}}{\varepsilon}. \quad (6)$$

We note that the focal strength k varies with particle momentum so that the beam size Σ, and its variation with the quadrupole magnet setting, thus depend on the beam momentum distribution. In order to obtain the beam size resulting from the momentum distribution we need to integrate Eq. (5) over all momenta, weighted by the momentum distribution function $\psi(\delta)$

$$\Sigma^2 = \int \Sigma(\delta)^2\psi(\delta)d\delta = A\sigma_{11} + B\sigma_{12} + C\sigma_{22}. \quad (7)$$

The factors A, B and C in the equation system are thus modified as the momentum spread grows and consequently the extracted parameters σ_{ij} will differ as well. An illustration of this chromatic effect is presented in Fig. 3 where the beam sizes during a quadrupole scan have been computed for a monochromatic beam and a beam with Gaussian momentum distribution with rms spread 0.1 and 0.2. More details can be found in Ref. [5].

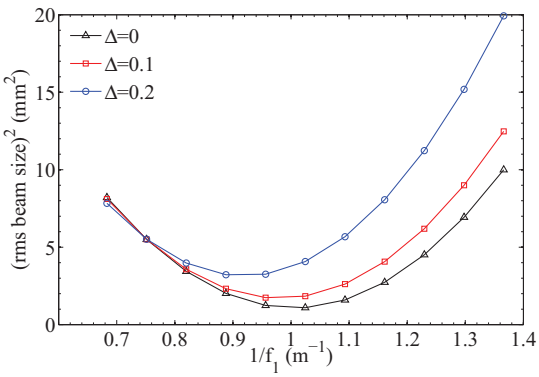

Figure 3: Beam sizes during a synthetic quadrupole scan for a monochromatic beam and a beam with Gaussian momentum distribution of rms width 0.1 and 0.2.

In Ref. [6] we have studied in detail the effect of chromaticity on quadrupole scan emittance measurements and offer an algorithm for analyzing quadrupole scan measurements that takes the momentum spread into account. It is instructive to use the thin-lens approximation of the quadrupole magnets. In the algorithm we have chosen a beamline model with two quadrupole magnets separated by a drift, and followed by another drift and a beam size measurement device. For simplicity, we let the strength of the second quadrupole be fixed while the strength of the first quadrupole is varied. The matrix elements R_{ij} will then be a function of the focal length $f = 1/(kl)$ where k is the strength and l the effective length of the magnet.

We introduce the momentum dependence by $f = (1+\delta)f_0$ with f_0 being the focal length for a given magnet setting corresponding to a particle with momentum p_0. Writing R_{11}^2, $R_{11}R_{12}$ and R_{12}^2 explicitly we see that they can be separated into terms of inverse powers of f, up to the fourth order. As we perform the integration in Eq. (7) we note that, with the stated parametrization of f, the momentum dependence can be isolated in integrals of the form

$$I_n = \int \frac{\psi(\delta)}{(1+\delta)^n}d\delta \quad n = 1, 2, 3, 4. \quad (8)$$

ISBN 978-3-95450-127-4

These integrals can be computed numerically for almost any momentum distribution ψ. That enables us to compute new matrix elements A, B, C that correspond to the evolution of the beam envelope for that given momentum distribution. These adjusted matrix elements are new factors in the system of equations which can then be solved and the incoming Twiss parameters determined correctly.

Figure 4 shows the result of a synthetic quadrupole scan made on a beam with Gaussian momentum profile of increasing rms width Δ. The Twiss parameters extracted using the conventional monochromatic model diverge significantly from the real Twiss parameters as the momentum spread grows. The input parameters are recovered if the momentum spread is taken into account in the analysis, as described above.

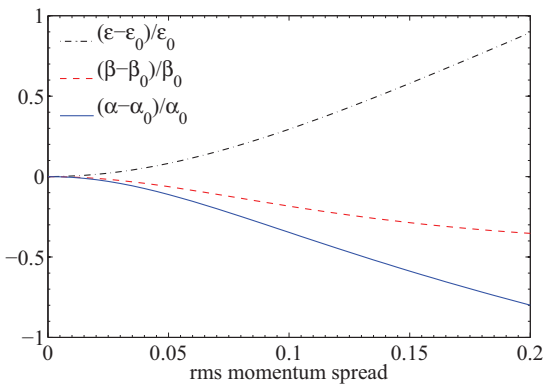

Figure 4: Twiss parameters extracted from a synthetic quadrupole scan using the monochromatic model. As the rms momentum spread Δ increases the extracted values diverge from the true values.

The beam emittance and Twiss parameters can also be extracted from a multiple-screen measurement. In the multiple-screen method the beamline optics is fixed and the beam size is measured in at least three different locations. Similarly to the quadrupole scan the method results in a system of equations in σ_{ij} with a different transfer matrix R for every screen. Also the multiple-screen method is subject to chromatic effects, which we have studied and described in Ref. [6].

We have described how to correctly analyze both spectrometer measurements and emittance measurements in the presence of large momentum spread. This will be of utmost importance in the CLIC drive beam decelerator where extraction of up 90% of the initial energy leaves the beam with a highly asymmetric momentum profile with a very large spread.

THE POST-PETS LINE

In the CLIC drive beam decelerator we want to access the momentum profile along each bunch train after the power extraction and transfer structures (PETS). For this purpose we suggest the Post-PETS line; a diagnostic section consisting of a fast sweeping magnet and an OTR screen. The magnet should deflect the beam in two transverse dimensions simultaneously and steer it onto the screen as a Lissajous figure. We assume that the magnet can be cycled in a way such that the particle coordinates on the screen are

$$X = \frac{L\varphi_0 \cos(2\pi\tau)}{1+\delta}\,, \quad Y = \frac{L\varphi_0 \sin(2\pi\tau)}{1+\delta} \tag{9}$$

with the arrival time $\tau = t/T$ and T being the cycle period of the magnetic deflection. With a period on the order of 300 ns the bunch train is sprayed on the screen along a circle, but with the head of the bunch train well separated from the tail. Similarly to Eq. (2) we can calculate the two-dimensional spatial distribution $\Psi(X,Y)$ on the screen by integrating over time and momentum weighted by the momentum distribution in time $\psi(\tau,\delta)$. The result is

$$\Psi(X,Y) = \frac{L\varphi_0}{2\pi}\frac{1}{(X^2+Y^2)^{3/2}}\,\psi\left(\tau(X,Y),\delta(X,Y)\right) \tag{10}$$

with

$$\tau(X,Y) = \frac{1}{2\pi}\arctan\left(\frac{Y}{X}\right) \tag{11}$$

$$\delta(X,Y) = \frac{L\varphi_0}{\sqrt{X^2+Y^2}} - 1\,. \tag{12}$$

In the conversion from one two-dimensional parameter space to another in Eq. (10) we use the Jacobi determinant which results in the scaling factor in front of ψ. Note that the momentum variable is now encoded in the radial direction on the screen, while the time along the bunch train lies in the angle with a reference axis. In this way the two variables are completely separated in a way that is not possible with a linearly rising magnetic deflection in one direction. An example of this is shown in Fig. 5 where the momentum distribution in the CLIC decelerator has been converted into spatial distribution for different dispersions D, corresponding to different points in time along the bunch train. The large spread leads to overlapping of the late bunches with the early bunches [4].

In order to extract the time-resolved momentum distribution from the spectrometer measurement we need the inverse procedure, which reads

$$\psi(\tau,\delta) = \frac{2\pi\,(L\varphi_0)^2}{(1+\delta)^3}\,\Psi\left(X(\tau,\delta),Y(\tau,\delta)\right)\,, \tag{13}$$

with $X(\tau,\delta)$ and $Y(\tau,\delta)$ as defined in Eq. (9).

Using these analytical transformations we investigate what the decelerated CLIC drive beam would look like in the Post-PETS Line. We use a momentum distribution obtained with PLACET [7], presented in Ref. [6] (Fig. 7). We use the peak energy of 240 MeV as a reference energy and ignore the high-energy transient, implying that the value of δ will vary between 0 and 4. We further let the momentum distribution be constant along the 240 ns bunch train and choose a sweeping period of 300 ns. The initial momentum

ISBN 978-3-95450-127-4

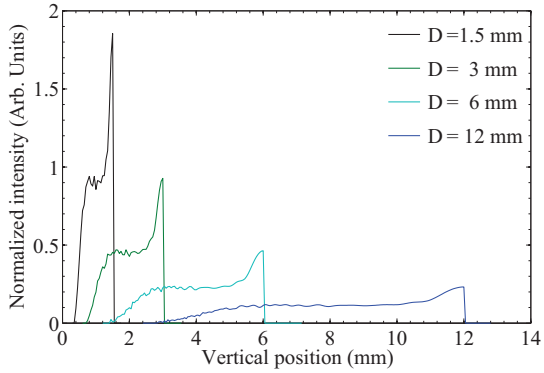

Figure 5: The momentum distribution in the CLIC decelerator converted into spatial distribution for different dispersions D.

distribution over time is presented in Fig. 6. With $L = 5\,\mathrm{m}$ and $\varphi_0 = 1.5\,\mathrm{mrad}$ the beam distribution will appear on the screen as in Fig. 7. The increase in intensity close to the center of the screen appears because of the singularity in the scaling factor from the Jacobi determinant, which was also pointed out in Eq. (2) for the one-dimensional case.

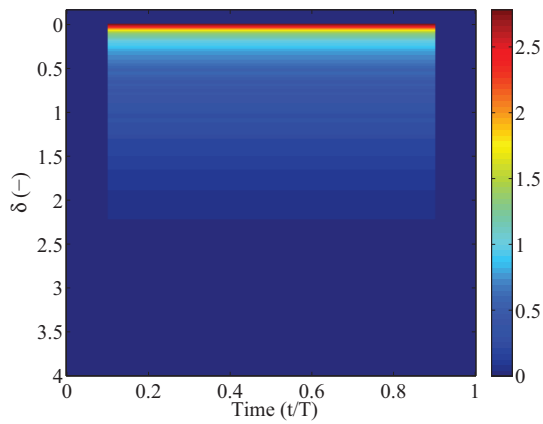

Figure 6: Two-dimensional momentum distribution.

The momentum distribution along the bunch train can be extracted from the spatial distribution in Fig. 7 using Eq. (13) and thus the distribution in Fig. 6 is recovered.

A non-zero emittance will appear as a smearing of the spectrometer image. If the intrinsic beam size is known it should be possible to correct for this through a two-dimensional deconvolution with the geometric beam profile. Since that is not a trivial procedure different image processing techniques have been envisioned for this step [4]. In the CLIC case, however, the intrinsic beam size is negligible compared to the beam size due to momentum spread.

CONCLUSIONS

Some standard beam diagnostic methods assume a very small beam momentum spread, which is not always a valid assumption. We have investigated how large momentum spread leads to systematic misinterpretations of profile measurements, with the CLIC drive beam decelerator in mind. Furthermore, we have presented a non-perturbative method to analyze spectrometer measurements, valid for arbitrary momentum distributions. We have developed an algorithm to correctly analyze emittance measurements through quadrupole scans which take the full momentum distribution and chromatic effects into account. For the CLIC drive beam decelerator we propose the post-PETS line, which relies on a fast sweeping magnet that deflects the beam in the two transverse directions, in a circular motion onto an OTR screen. In this way the momentum distribution can be read out along every bunch train from the particle density in the radial direction and the angular direction.

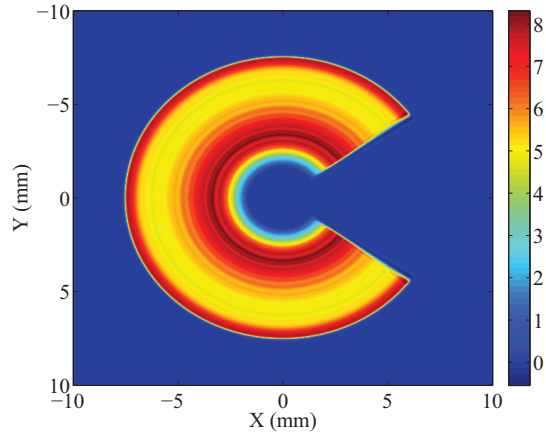

Figure 7: The momentum distribution in Fig. 6 projected on a screen with $L = 5\,\mathrm{m}$ and $\varphi_0 = 1.5\,\mathrm{mrad}$.

REFERENCES

[1] CLIC conceptual design report, (2012). CERN-2012-007.

[2] I. Blumenfeld et al. *Nature*, 445:741–744, (2007).

[3] A. Mostacci et al. *Phys. Rev. ST Accel. Beams*, 15:082802, Aug 2012.

[4] M. Olvegård. *Emittance and Energy Diagnostics for Electron Beams with Large Momentum Spread*. PhD thesis, University of Uppsala, Uppsala, Sweden, (2013).

[5] M. Olvegård et al. *Phys. Rev. ST Accel. Beams*, 16:082802, Aug 2013.

[6] M. Olvegård and V. Ziemann. *Nucl. Instrum. and Methods A*, 707(0):114 – 119, (2013).

[7] D. Schulte. PLACET: a program to simulate drive beams. CERN-PS-2000-028 AE.

ISBN 978-3-95450-127-4